DOI: https://doi.org/10.1016/j.jms.2014.11.003

Analysis of the Rotation-Vibration-Inversion Far Infrared Spectrum of the ν_{10} and ν_{14} Bands of Silacyclobutane

Ziqiu Chen and Jennifer van Wijngaarden*

Department of Chemistry, University of Manitoba, Winnipeg Manitoba, R3T 2N2 Canada

*Corresponding author

Email: vanwijng@cc.umanitoba.ca

Phone: (204)474-8379

Fax: (204)474-7608

Abstract

Fourier transform spectra of the four-membered heterocycle silacyclobutane (c-C_3H_8Si)(SCB) were recorded in the far infrared region from 500-800 cm^{-1} with a resolution of 0.000959 cm^{-1} using synchrotron radiation from the Canadian Light Source. Two fundamental bands observed in this region have been rotationally analyzed. These correspond to motions best described as the in-plane ring deformation mode (ν_{10}) at ~543 cm^{-1} and the α-CH_2 rocking mode (ν_{14}) at ~737 cm^{-1}. Both bands exhibit complex, dense spectral patterns that arise from ring inversion tunnelling of the puckered SCB ring through a planar (C_{2v}) intermediate configuration. Analysis of these patterns revealed rotation-vibration transitions between states of the same inversion symmetry for the ν_{10} mode as well as rotation-vibration-inversion transitions that connect states of different inversion symmetry. Only rotation-vibration-inversion transitions are observed in the ν_{14} band due to symmetry as the vibration (A_2) is IR forbidden. In total, 12 371 far infrared transitions were assigned for the ring deformation and α-CH_2 rocking bands and combined with those from analysis of the ring puckering (158 cm^{-1}) and SiH_2 rocking modes (410 cm^{-1}) [J. Chem. Phys. 139, 244305 (2013)]. A 10 state fit was performed from the resulting data set containing 20 626 rotation-vibration-inversion transitions and provided accurate band centers, ring inversion splittings, rotational and centrifugal distortion constants for the lowest energy states of the dynamic silacyclobutane ring.

KEYWORDS: rovibrational spectroscopy; ring inversion; ring puckering; synchrotron; far infrared; silacyclobutane

1. Introduction

Silacyclobutane (c-C_3H_8Si)(SCB) and its derivatives have been explored as starting materials for the production of organosilicon materials such as silicon carbide films.[1,2,3,4] Compared with other potential precursors, the decomposition of silacyclobutane is facilitated by the high ring strain in the four-membered ring backbone.[5] The relationship between the structure and stability of a compound is governed by its potential energy surface and can be explored using various spectroscopic techniques. The far infrared spectra of small heterocycles, for example, provide information about the lowest energy states of these systems and have been the subject of numerous reviews.[6,7,8]

In recent years, we have reported high resolution spectroscopic investigations of SCB in both the microwave[9] and far infrared[10] regions with the latter focusing on vibrations below 500 cm^{-1}. Although such four-membered rings have been under spectroscopic scrutiny for half a century, modern techniques have enabled the study of molecules such as SCB with greater detail. For example, the equilibrium geometry of SCB is that of a puckered ring backbone (Figure 1) with a barrier to planarity of ~440 cm^{-1}.[11,12] Evidence of ring inversion tunnelling through this barrier is observed in the pure rotational spectrum of SCB using Fourier transform microwave (FTMW) spectroscopy and this splitting was observed in the ground state for the first time in 2011.[9] This splitting was only 10 kHz for the lowest transition and thus inaccessible in earlier microwave studies.[12] In the far infrared region, synchrotron radiation has shown great promise as a light source for measurements below 1000 cm^{-1} when spectral resolution of 0.001 cm^{-1} or better is needed.[13] Spectra of this type have been used, for example, to derive the ring puckering potential of 3-oxetanone (c-$C_2H_4(CO)O$)[14] using its hotbands at ~140 cm^{-1} and also to

characterize the coupling of NH inversion tunnelling with the ring puckering vibration of azetidine (c-C_3N_6NH)[15] at ~208 cm^{-1}.

The low-resolution vibrational spectrum of SCB has been well-studied using infrared and Raman methods.[11,16,17,18] Based on DFT calculations in 2008, nine of the previously studied fundamental bands were re-assigned.[18] Similar discrepancies are not uncommon in the literature and while computational techniques are now playing a larger role in vibrational assignments, rotationally-resolved spectra provide irrefutable, experimental evidence for correcting such mis-assignments. We recently reported the first such study of SCB and described the assignment of 8 255 far infrared transitions corresponding to the weak ν_{30} ring puckering (~158 cm^{-1}) and medium intensity ν_{29} SiH_2 rocking (~410 cm^{-1}) vibrations using spectra recorded at room temperature at the Canadian Light Source.[10] Both vibrational bands have B_1 symmetry which leads to *c*-type rotational structure and in the high resolution spectrum, these rotation-vibration transitions were observed to be doubled due to ring inversion tunnelling. By symmetry, transitions that cross between inversion states of opposite parity are also allowed and are expected to follow *a*-type selection rules. The observed structure of the ν_{29} band confirmed the presence of these rotation-vibration-inversion transitions but the analogous features were not observed for the ring puckering band due to the low signal. In the end, the assigned transitions of the ν_{29} and ν_{30} bands spanned energy levels with quantum numbers up to J=52 which allowed the determination of a set of accurate spectroscopic constants for the ground and both excited vibrational states including the band origins . The energy gap between the inversion components of each vibrational level was also unambiguously determined due to the observation of rotation-vibration-inversion transitions in the ν_{29} band in particular. The resulting ground state parameters

were much improved over those based on FTMW measurements as the latter were recorded at low rotational temperatures in a supersonic jet and thus sampled energy levels up to only J=3.[9]

The present article describes the collection and analysis of a rotationally-resolved infrared spectrum of SCB above 500 cm^{-1}, which was collected at the Canadian Light Source synchrotron. We detail the symmetry considerations needed to understand the spectra of modes belonging to both A_1 and A_2 (IR forbidden) irreducible representations and invoke these selection rules to analyze the dense spectral patterns of the ν_{10} ring deformation and the ν_{14} α-CH_2 rocking motions at ~543 cm^{-1} and ~737 cm^{-1}, respectively. The rotational structure of these bands reveals the presence of ring inversion tunnelling and our analysis accounts for both rotation-vibration and rotation-vibration-inversion transitions in this spectral range. Following individual band analysis, the assigned frequencies were added to those reported for the ν_{30} ring puckering and ν_{29} SiH_2 rocking below 500 cm^{-1}.[10] The resulting data set consists of 20 626 lines and was used to derive accurate spectroscopic constants for each of the ground and four excited vibrational states as well as their ring inversion tunnelling splittings.

2. Experimental details

SCB is not commercially available and thus, the sample was prepared by a one-step reduction[16] of 1,1-dichlorosilacyclobutane (GELEST, 97%). This precursor was mixed with $LiAlH_4$ in a 2:1 ratio in *n*-butyl ether for 24 h. The final product was distilled from the mixture at 110 °C using a dry ice/acetone-cooled receiving flask and verified by GC/MS.

The rovibrational spectra of SCB were collected at the Canadian Light Source (CLS) using synchrotron light as the source for a high resolution Fourier transform infrared (FTIR) spectrometer (Bruker IFS125HR). The low pressure gas sample was prepared by introducing

vapour from the liquid sample into a multipass gas cell. Although various optical set ups are available on site, the spectra of the ν_{10} and ν_{14} bands were recorded using a KBr beamsplitter and a helium-cooled GeCu detector and a total absorption path length of 72 m through the multipass 2 m gas cell. A total of 426 interferograms were recorded at a resolution of 0.000959 cm^{-1} over 42 hours at a sample pressure of 35 mTorr.

3. Symmetry considerations

As described in our earlier study of SCB,[10] the molecular symmetry group C_{2v} is needed to describe the ring inversion tunnelling that interconverts the equivalent puckered C_s equilibrium structures as shown in Figure 1. The barrier to planarity is 440 cm^{-1} (reference 11,12) along the ring puckering coordinate and as a result of tunnelling, the ground vibrational state is split into two components (0^+ and 0^-) which can be labelled with the inversion part of the wavefunction (B_1) (if the ring lies in the yz plane). In this study, the vibrational bands under consideration are the in-plane ring deformation (ν_{10}) with A_1 symmetry and the out-of-plane α-CH_2 rocking motion (ν_{14}) with A_2 symmetry. The rotational part of the wavefunction under C_{2v} symmetry can be categorized by whether K_a and K_c are even (e) or odd (o) and can be classified by the A_1 (ee), A_2 (eo), B_1 (oo) or B_2 (oe) irreducible representations under C_{2v}. To determine the symmetry selection rules, one must consider the direct product of the symmetries of the various parts of the wavefunction ($\Gamma_{rot}\times\Gamma_{vib}\times\Gamma_{inv}$) which can be used to label each rotational sublevel in the ground (0) and excited (1) vibrational states under consideration. Transitions are allowed if the product contains the totally symmetric irreducible representation (A_1) when combined with the symmetry of the space-fixed molecular dipole moment (A_2). A summary of the symmetries of the various energy levels and allowed transitions is provided in schematic form in Figures 2 and 3 for the ν_{10}

or ν_{14} bands, respectively. For the ν_{10} band in Figure 2, the spectrum is predicted to contain two sets of *a*-type rotation-vibration transitions ($0^+ \rightarrow 1^+$, $0^- \rightarrow 1^-$) that connect states of the same inversion parity superimposed with two sets of *c*-type rotation-vibration-inversion transitions ($0^- \rightarrow 1^+$, $0^+ \rightarrow 1^-$) that connect states of opposite inversion parity. By comparison, the rotation-vibration transitions are symmetry forbidden for the ν_{14} band leading previous studies to declare that the A_2 vibrations are infrared inactive.[17,18] A spectrum in this region is expected, however, as two sets of *b*-type rotation-vibration transitions connecting states with opposite inversion parity are allowed by symmetry as shown in Figure 3.

4. Spectral assignment and analysis

Initially, the observed rotationally-resolved transitions in the ν_{10} and ν_{14} bands of SCB were assigned and fit separately using Watson's A-reduced Hamiltonian in I^r representation in Pickett's SPFIT program.[19] Eventually, transitions from both bands were combined with those of the previously reported ν_{29} and ν_{30} bands in a global analysis to obtain the final set of spectroscopic constants. The assignment and analysis are detailed below.

a) ν_{10} band

The ν_{10} band centered at ~543 cm^{-1} is attributed to an in-plane ring deformation and the overall band contour is shown in Figure 4. No obvious patterns were observed in the initial visual inspection of the rotational structure of this band. To identify regularly spaced progressions, the most intense transitions between 520 and 565 cm^{-1} were used to construct a Loomis-Wood plot using a software add-in for Igor Pro.[20,21] As shown in Figure 5, R branch transitions of this band are grouped in such a way that those sharing common K_a quantum

numbers but having different J values are arranged in a vertical series of K_a on the Loomis-Wood plot. These correspond to strong *a*-type progressions that connect vibrational levels of the same inversion symmetry ($0^+ \rightarrow \nu_{10}^+$ and $0^- \rightarrow \nu_{10}^-$) and the tunnelling splitting is marked with a double-headed arrow. The observed spectral pattern was then compared with the simulated rotation-vibration spectrum (based on the estimated band origins and the ground state constants determined from our previous study),[10] leading to the tentative assignment of a few of the strongest infrared transitions. Ground state combination differences (GSCDs) confirmed the assignment of these *a*-type transitions. The simulated spectrum was then refined and the assignment process continued in an iterative manner until the strongest progressions were included.

After the assignment of the *a*-type lines, obvious strong features remained unassigned that were not part of an obvious progression in the Loomis-Wood plot shown in Figure 5. As two *c*-type bands were also expected based on symmetry, new Loomis-Wood plots were constructed in an attempt to identify additional progressions. Unfortunately, the increment required to observe the repeating pattern of common K_c progressions was nearly exactly double that needed to observe the common K_a progressions of the *a*-type bands which created a congested plot that was dominated by previously-assigned transitions. Based on the simulation of both the *a*-type and *c*-type transitions, it was found that the *c*-type progressions were stronger than the a-type transitions toward the band edges and thus, the initial assignment focused on these regions. A second plot of the R branch given in Figure 6 shows the progressions of common K_c that were used to identify the *c*-type rotation-vibration-inversion bands. Note that these become visible as the more pronounced *a*-type progressions (near the top of the plot) wane in intensity. Note that the period (x-axis) depicted in this plot is about double that in Figure 5 so that the J labels along

the y-axis are about half of those needed for the correct J assignment in the *a*-type bands. As the transition intensities were lower at the edge of the bands and the tunnelling splitting between the excited vibrational states was not well-determined from the preceding *a*-type band analysis, it was difficult to identify extended progressions in both P and R branches of the *c*-type bands to make a convincing assignment from GSCDs. Thus, a third Loomis-Wood plot was created to illustrate series of common K_a within the *c*-type bands and this is shown in Figure 7. The use of this additional plot is that it clarifies the relationship between the series identified in Figure 6 and 7. The colours have been chosen to illustrate their correspondence. For example, progressions of common K_a in Figure 7 start with a red or yellow triangle to correspond to those with K_c=0 from Figure 6; the next transition is labelled as either lime or pink (K_c=1); and the next as either blue or brown (K_c=2). The progressions labelled as K_a=26 in Figure 7 would thus consist of transitions with upper states (J K_a J_c) as (26 26 0), (27 26 1) and (28 26 2) in each tunnelling state. This relationship between Figures 6 and 7 is mirrored in the R-branch and helped to identify the leading lines of *c*-type progressions with confidence. The assignment of the tunnelling doubled *c*-type progressions followed the same procedure as for the *a*-type spectrum and ground state combination differences were closely tracked to avoid mis-assignment. A portion of the P-branch spectrum is shown in Figure 8 to demonstrate the complexity of the rotation-inversion structure caused by the four overlapping bands.

Overall, 7 652 transitions from the ν_{10} band were assigned and fit: 3 552 *c*-type transitions and 4 100 *a*-type transitions. The quantum number coverage of the assigned lines is listed in Table 1. Analysis of the Q branch was not attempted as the spectrum in this region was too dense and largely saturated.

b) ν_{14} band

The ν_{14} band at ~737 cm^{-1} corresponds to the α-CH_2 rocking motion of SCB. Initial inspection of the band contour shows a typical *b*-type envelope without a central Q branch feature as shown in Figure 9. Although this band has been reported in low resolution studies,[17,18] it is an IR forbidden vibration and is only observed because of the presence of ring inversion tunnelling in SCB. The observed features are thus rotation-vibration-inversion transitions. A Loomis-Wood plot was constructed to aid in the initial stages of the assignment and two sets of progressions were soon identified as the *b*-type transitions connection states of the opposite inversion symmetry ($0^+ \rightarrow \nu_{14}^-$ and $0^- \rightarrow \nu_{14}^+$) of SCB. The assignment scheme described above for the ν_{10} band was implemented and overall, 4 719 *b*-type transitions were assigned in this region including 706 Q branch transitions. The coverage of rotational levels is shown in Table 1.

c) Global analysis

The 12 371 transitions assigned for the ν_{10} ring deformation and ν_{14} α-CH_2 rocking bands were combined with those reported for the ν_{29} SiH_2 rocking and ν_{30} ring puckering bands to produce a data set with 20 626 transitions describing the ground state and four excited vibrational states as well as the ring inversion tunnelling splittings of each of these states. The vibrational modes sampled in this set include states of A_1 (ν_{10}), A_2 (ν_{14}) and B_1 (ν_{29}, ν_{30}) symmetry, respectively leading to three different sets of selection rules to characterize their rotation-vibration-inversion spectra. All assigned transitions from the four bands were incorporated into a global fit using Watson's A-reduced Hamiltonian, I^r-representation in SPFIT.[19] The rms error of the resulting simultaneous 10 state fit was 0.000 161 cm^{-1} and the

determined spectroscopic constants are listed in Table 2. The complete list of all assigned rovibrational transitions is provided as Supplementary Information to this article.

4. Discussion

The previous far infrared spectroscopic study[10] on SCB proved invaluable in the analysis of the dense far infrared spectrum of the ν_{10} and ν_{14} bands of SCB. The ground state of SCB was well-determined via fitting 1871 sets of GSCDs collected from the ring puckering (ν_{30}) and SiH_2 (ν_{29}) rocking bands below 500 cm^{-1}. Both are of B_1 vibrational symmetry and exhibited *c*-type rovibrational structure although *a*-type rotation-vibration-inversion transitions were also assigned for the ν_{29} band. The final set of GSCDs thus contained both sets of selection rules and included rotational energy levels up to J=52 and K_a=40. Fitting of this data set provided an accurate description of the 0^+ and 0^- states and the energy splitting due to inversion. These parameters were critical for confirming the preliminary assignments of far infrared transitions in the present work for the bands above 500 cm^{-1}.

The observed far infrared spectra of the ν_{10} and the ν_{14} bands exhibit a rich rotational structure due to the presence of ring inversion tunnelling and our analysis provides confirmation of the symmetries involved in the various motions as detailed in Figures 2 and 3. Based on these symmetry considerations, it was possible to assign over 12 371 new infrared transitions for SCB in the range above 500 cm^{-1}. Of particular note is the assignment of two sets of *b*-type progressions due to the rotation-vibration-inversion spectrum of the ν_{14} band. This band was reported in earlier low resolution infrared studies[17,18] even though it was said to be IR forbidden and we now show a clear explanation for this observation.

The assignment of structure in the ν_{10} and ν_{14} bands involve rotational levels with high J and K_c values (up to 64) which provides good coverage of these vibrational manifolds and adds new information about the ground vibrational state. When combined with the previous data set for the ν_{29} and ν_{30} bands,[10] 20 626 transitions were fitted to a standard Hamiltonian (Watson's A-reduced Hamiltonian, I^r-representation) without required sextic (or higher order) distortion constants or perturbation terms. The rms error of the fit is remarkably low (0.000 157 cm^{-1}). The parameters are well determined and consistent in sign and magnitude across all states as shown in Table 2. Furthermore, this model accounts for all observed P and R branch transitions of reasonable intensity in this spectral region as demonstrated in Figure 8 for the ν_{10} ring deformation mode.

The ground state spectroscopic parameters determined in the present work are compared in Table 3 with those derived solely from the GSCDs reported in reference 10 which served as our initial estimates of the rotational structure and inversion splitting of the ν_{10} and ν_{14} bands. Using GSCDs to derive the ground state parameters is useful when there are perturbations in the excited state as one can isolate these effects and treat them once the ground state properties are established. In the case of SCB, perturbations have not been encountered for the four far infrared bands studied to date and the determination of the ground state parameters in the present work was thus done via the global infrared analysis where all parameters in Table 2 were varied simultaneously. The resulting spectroscopic constants for the ground state are in good agreement with those reported earlier via GSCDs and generally agree to within 2σ. The uncertainties in the ground state parameters from the present analysis are smaller which makes it appear that the ground state is better determined. This arises partially from the inclusion of higher energy levels

(J, K_c up to 64 in some cases) but is also an artificial consequence of the fit as more parameters are varied in the global infrared analysis.

The band origins of the ν_{10} (543.392617(12) cm^{-1}, 543.312870(11) cm^{-1}) and ν_{14} (737.272771(16) cm^{-1}, 737.287075(11) cm^{-1}) modes of SCB were accurately determined for the first time. As both bands feature rotation-vibration-inversion transitions that connect states of different inversion symmetry, the relative ordering of the inversion components in the ν_{10} and ν_{14} vibrational states was unambiguously determined. The inversion splitting of the energy levels of the ring deformation excited state was found to be 0.079747(23) cm^{-1} which is 30 times larger than the inversion splitting in the ground state of SCB (0.002531(10) cm^{-1}) and about six times larger than for the α-CH_2 rocking mode (0.014304 (26) cm^{-1}). In general, the smaller the energy gap between the inversion components is, the more similar are the spectroscopic parameters of the two states. In Table 2 for example, the ground state parameters agree to within the 1σ uncertainty of the constants from the fit of the 0^+ and 0^- states whereas the rotational constants for the ν_{29}^+ and ν_{29}^- states (which are split by 0.173857(20) cm^{-1}) differ by up to 160 times the 1σ the uncertainty of the parameters.

The experimental values for the band origins of all fundamental vibrations of SCB have been previously reported based on the low resolution spectra of Laane and co-workers.[17,18] The band origin of the ν_{14} vibration (~737 cm^{-1}) in the present study is consistent with these earlier reports but interestingly, the ν_{10} band is 11 cm^{-1} higher than previously reported. Although there is a weak Q branch feature in Figure 4 appearing near 532 cm^{-1} (the band origin identified by Laane and co-workers), we are confident that the ν_{10} fundamental band is centered near 543 cm^{-1}. This assertion is based on both the observed intensity of this feature as compared with predicted IR intensities from calculations[10,18] as well as on the assigned rotational structure. A fit of the

GSCDs from the *a*-type and *c*-type transitions of this band alone are wholly consistent with the feature centered at 543 cm^{-1} being a fundamental band of SCB. As we have previously reported the spectroscopic constants of the lowest frequency ring puckering vibration at 158 cm^{-1} also, we can further eliminate the possibility that this band at 543 cm^{-1} arises from a hotband feature originating from an excited ring puckering vibrational state.

The vibrational spectrum of SCB has been estimated via DFT and *ab initio* calculations using various basis sets, anharmonic corrections and empirical scaling factors.[10,18] In general, DFT calculations based on C_s symmetry provide the closest agreement across the infrared region of the spectrum with the largest discrepancies observed for the lowest frequency bands. The ring puckering fundamental band at 158 cm^{-1} was only predicted to within 8-20% for example.[10] For the two bands investigated in this work at 543 cm^{-1} and 737 cm^{-1}, the agreement is much better, however, with a standard DFT (B3LYP (6-311++G(2d2p) harmonic frequency calculation matching the band origins to within 2% (540 cm^{-1} and 750 cm^{-1}).[10] The anharmonic corrections for these bands do not provide systematic improvement (531 cm^{-1} and 735 cm^{-1}) and may suggest that the potentials governing these vibrations are fairly harmonic.

5. Summary

This article reports the first high resolution infrared spectroscopic investigation of the dynamic SCB molecule above 500 cm^{-1} using data from the Canadian Light Source synchrotron. The spectra are complicated by the presence of ring inversion which leads to tunnelling-doubled rotation-vibration transitions as well as tunnelling-doubled rotation-vibration-inversion transitions. The spectroscopic constants describing the ground state and the excited vibrational states corresponding to α-CH_2 rocking (ν_{14}) and ring deformation (ν_{10}) motions of this highly

fluxional molecule have been accurately determined for the first time. Through measurement of transitions that cross between states of opposite inversion symmetry, the energy difference and ordering of the tunnelling states was also derived. This study provides the foundation for further investigation of SCB in other wavelength regions and can be used by researchers who may seek to characterize the electronic structure of the silacylobutanes and thus better describe the chemistry of organosilicon-based materials.[3]

Acknowledgements

We extend our gratitude to B. Billinghurst for technical support at the Canadian Light Source. This research was funded by the Natural Sciences and Engineering Research Council of Canada (NSERC) through the Discovery Grants (JvW: RGPIN/326993-2010) and University Faculty Award (JvW) programs. We are grateful to the University of Manitoba for research fellowship support through the Faculty of Science and Faculty of Graduate Studies (ZC).

Supporting Information Available

The assigned transition frequencies for the two bands are provided as supplementary material. This information is available free of charge at:

Table 1: Quantum numbers of energy levels included in the spectral analysis of the ν_{10} and ν_{14} bands of SCB.

	$0^- \rightarrow \nu_{10}^+$	$0^+ \rightarrow \nu_{10}^-$	$0^- \rightarrow \nu_{10}^-$	$0^+ \rightarrow \nu_{10}^+$	$0^- \rightarrow \nu_{14}^+$	$0^+ \rightarrow \nu_{14}^-$
type	*c*	*c*	*a*	*a*	*b*	*b*
J(min)	5	4	7	6	4	3
J(max)	51	48	64	58	60	59
K_a(min)	1	1	0	0	0	0
K_a(max)	39	40	31	34	30	30
K_c(min)	0	0	1	1	0	0
K_c(max)	39	42	64	57	60	59
# transitions	1808	1744	2052	2048	2321	2398

Table 2: Spectroscopic constants for the ground state, ν_{10}, ν_{14}, ν_{29} and ν_{30} bands of SCB determined from rovibrational analysis.[a]

	0^+	0^-	ν_{30}^+	ν_{30}^-	ν_{29}^+	ν_{29}^-	ν_{10}^+	ν_{10}^-	ν_{14}^+	ν_{14}^-
ν / cm^{-1}	0	0.002538(9)	158.12185(2)	158.387197(15)	410.037573(10)	410.211433(10)	543.395156(11)	543.315408(11)	737.277841(13)	737.287077(15)
Rotational constants / cm^{-1}										
A	0.29406040(11)	0.29405945(12)	0.29364222(16)	0.29364648(13)	0.29394987(11)	0.29393364(12)	0.29368780(12)	0.29369138(12)	0.29384871(15)	0.29385126(14)
B	0.20977653(14)	0.20977683(13)	0.209489(2)	0.20946201(19)	0.20990242(15)	0.20990267(14)	0.20971053(14)	0.20970894(14)	0.20951616(15)	0.20951538(15)
C	0.14160684(9)	0.14160679(9)	0.140841(4)	0.1409261(3)	0.14136761(10)	0.14136628(10)	0.14164080(10)	0.14163924(10)	0.14146131(10)	0.14146272(10)
Centrifugal distortion constants / 10^{-9} cm^{-1}										
Δ_J	77.15(6)	77.48(6)	83.3(4)	79.87(17)	76.69(7)	76.48(7)	82.03(6)	81.98(6)	77.60(7)	77.03(7)
Δ_K	199.7(2)	203.8(2)	219.4(11)	216.5(7)	199.1(2)	201.9(2)	233.2(2)	230.5(2)	20.20(2)	19.74(2)
Δ_{JK}	-105.7(2)	-110.1(2)	-133.2(14)	-127.1(8)	-104.8(2)	-107.8(2)	-145.9(2)	-143.3(3)	-108.3(3)	-102.9(3)
δ_j	19.34(3)	19.58 (3)	19.26(14)	19.26[b]	19.71(3)	19.98(3)	17.44(3)	17.33(3)	19.62(3)	19.28(3)
δ_k	46.86(18)	46.14(18)	70.4(10)	70.4[b]	47.64(19)	45.66(19)	40.95(18)	42.72(18)	47.41(19)	47.67(19)
rms error /cm^{-1}	0.000161									

[a] Transitions from the ν_{29} and ν_{30} bands are from reference 10.

[b] Values held fixed to these of the ν_{30}^+ state.

Table 3: Comparison of ground state spectroscopic constants of SCB determined via ground state combination differences and the present rovibrational analysis.

	Current work		GSCD (reference 10)	
	0^+	0^-	0^+	0^-
A / cm^{-1}	0.29406040(11)	0.29405945(12)	0.2940600 (3)	0.2940595 (3)
B	0.20977653(14)	0.20977683(13)	0.2097760 (16)	0.2097752 (6)
C	0.14160684(9)	0.14160679(9)	0.1416060 (7)	0.1416076 (3)
Δ_J / 10^{-9} cm^{-1}	77.15(6)	77.48(6)	79.0(9)	79.8(4)
Δ_K	199.7 (2)	203.8(2)	207(3)	208.2(14)
Δ_{JK}	-105.7(2)	-110.1(2)	-115(4)	-117.0(17)
δ_J	19.34(3)	19.58 (3)	20.4(5)	20.55(19)
δ_K	46.86(18)	46.14(18)	51(3)	50.4(8)
ΔE /cm^{-1}	0.002538(9)		0.002665(6)	
# transitions	20626		1871	

Figure 1: Ground state geometry of silacyclobutane in its principal inertial axis system.

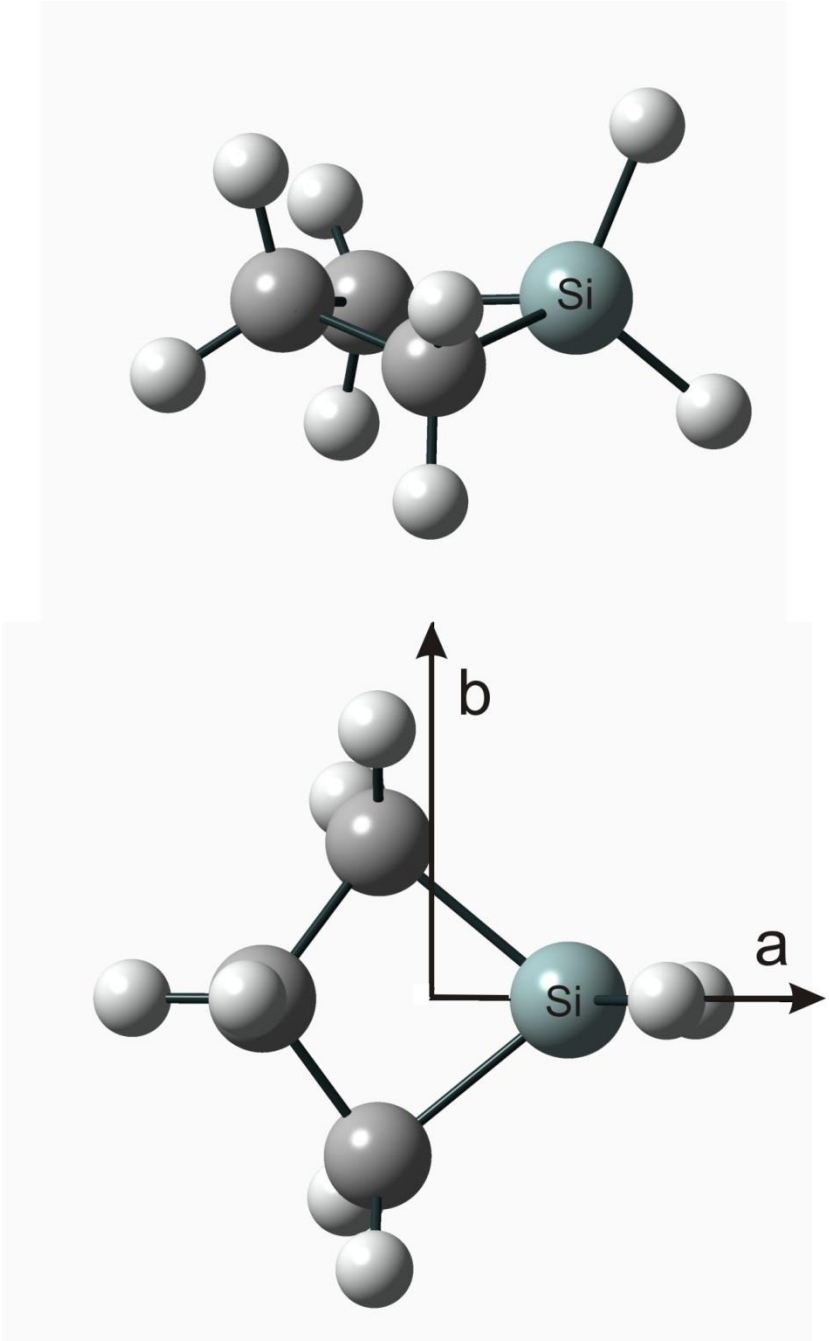

Figure 2: A schematic showing the symmetry-allowed transitions for the ν_{10} band of SCB. The rotational sub-levels (K_aK_c)(even/odd) are labelled with their rotation-vibration-inversion symmetry.

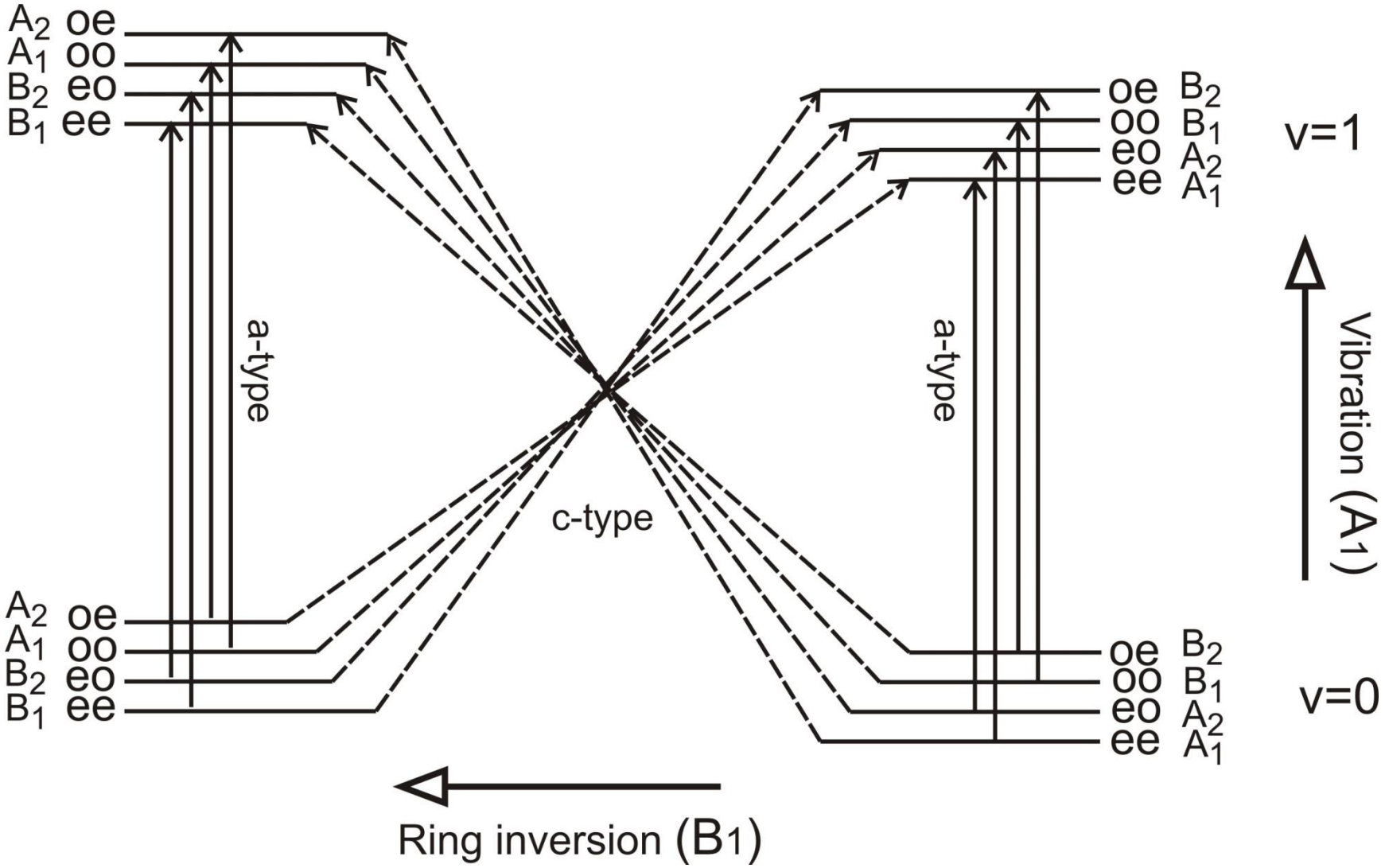

Figure 3: A schematic showing the symmetry-allowed transitions for the ν_{14} band of SCB. The rotational sub-levels (K_aK_c)(even/odd) are labelled with their rotation-vibration-inversion symmetry.

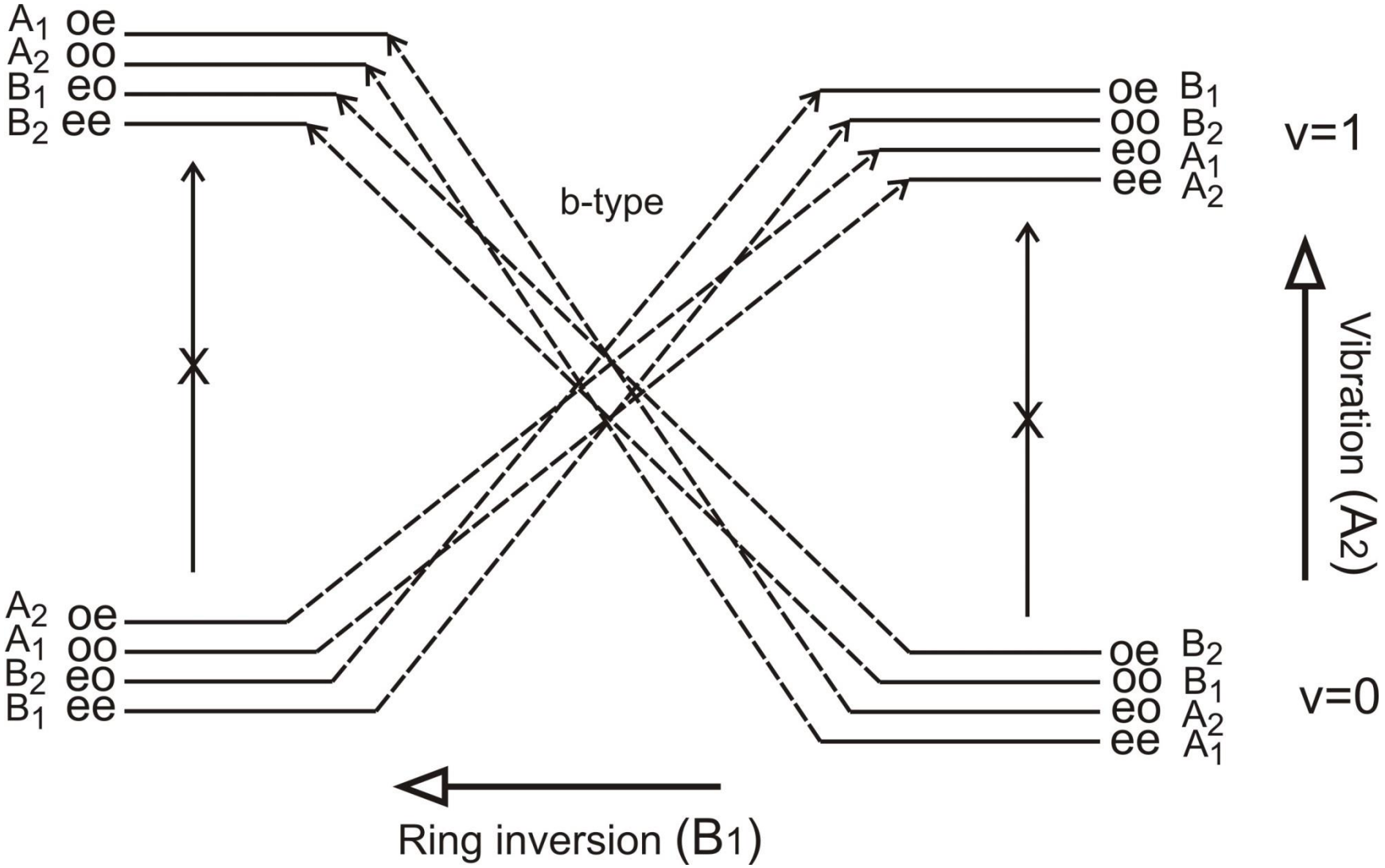

Figure 4: Overview spectrum showing band contour of the ν_{10} ring deformation mode of SCB at ~543 cm^{-1}. This spectral region contains four bands as described by the selection rules in Figure 2.

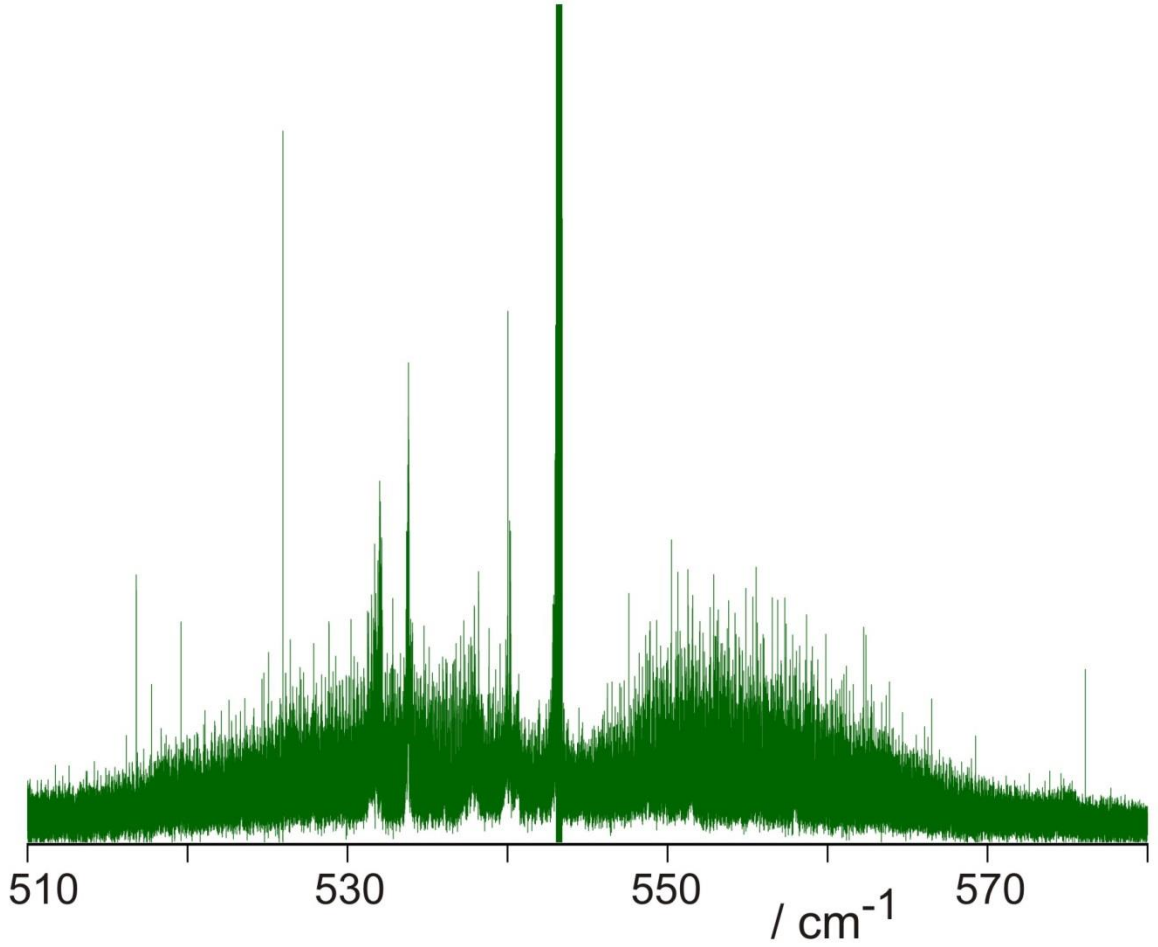

Figure 5: A portion of the Loomis-Wood plot of the ν_{10} band of SCB showing *a*-type progressions used to aid in its assignment. The coloured series identify transitions sharing common K_a but having different J values with $0^+ \rightarrow \nu_{10}^+$ and $0^- \rightarrow \nu_{10}^-$, respectively and the ring inversion tunnelling splitting is shown with double-headed arrows.

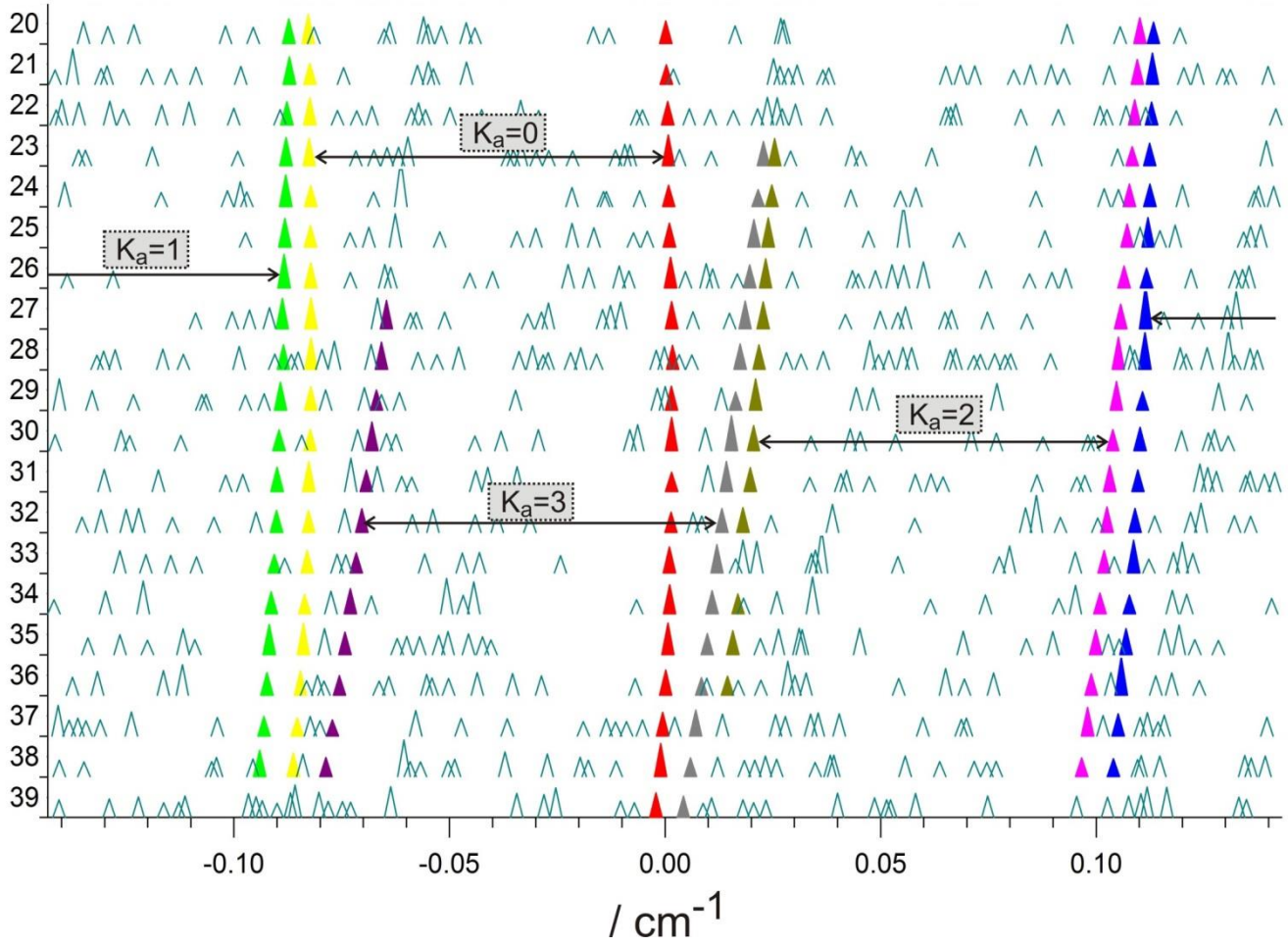

Figure 6: A portion of the Loomis-Wood plot of the ν_{10} band of SCB showing *c*-type progressions used to aid in its assignment. The coloured series identify transitions sharing common K_c but having different J values for the bands $0^+ \rightarrow \nu_{10}^-$ and $0^- \rightarrow \nu_{10}^+$, respectively. The ring inversion tunnelling splitting is shown with double-headed arrows.

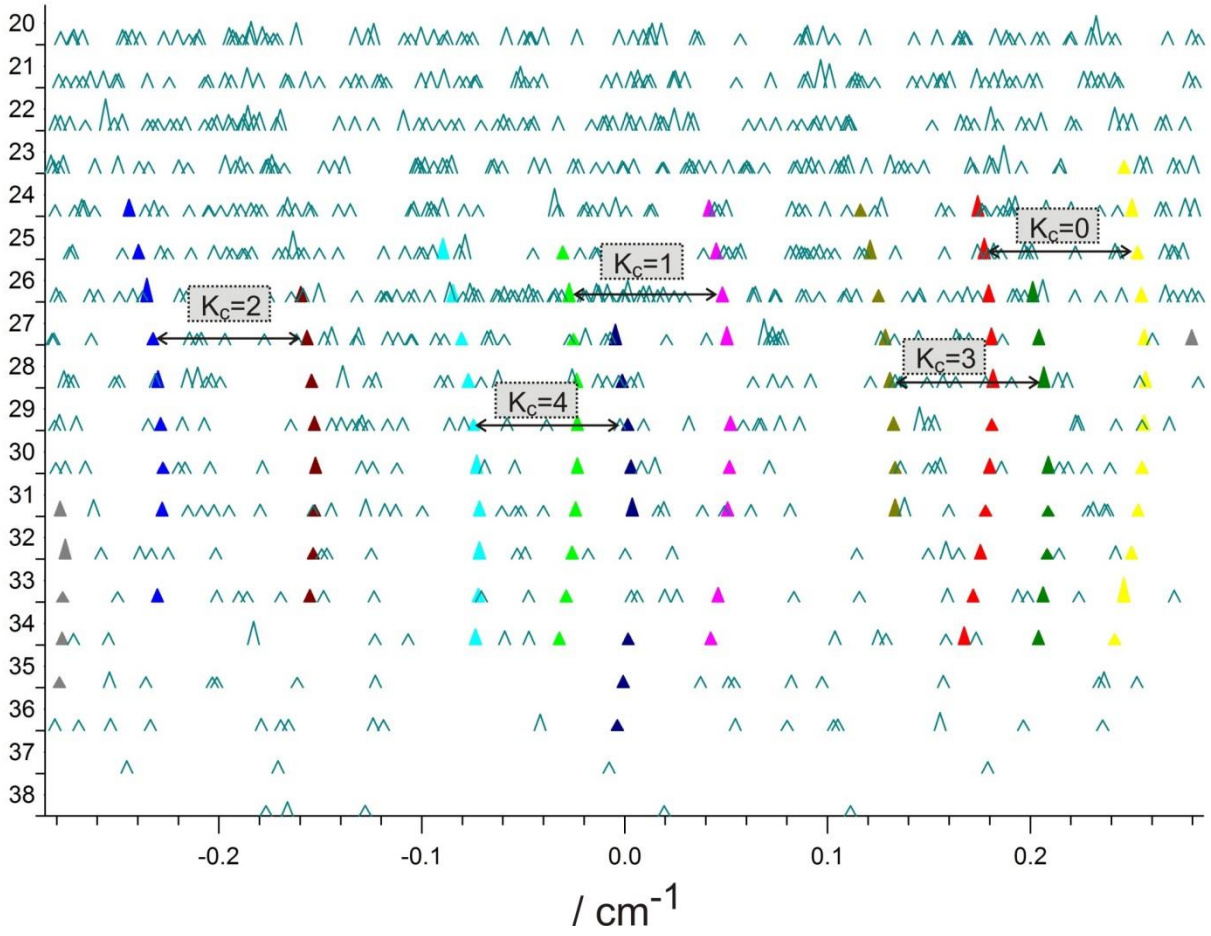

Figure 7: A portion of the Loomis-Wood plot of the ν_{10} band of SCB showing *c*-type progressions used to aid in its assignment. Each multi-coloured series identifies transitions sharing common K_a but having different J values. The colours are used to identify the value of K_c in Figure 6. The ring inversion tunnelling splitting is shown with double-headed arrows.

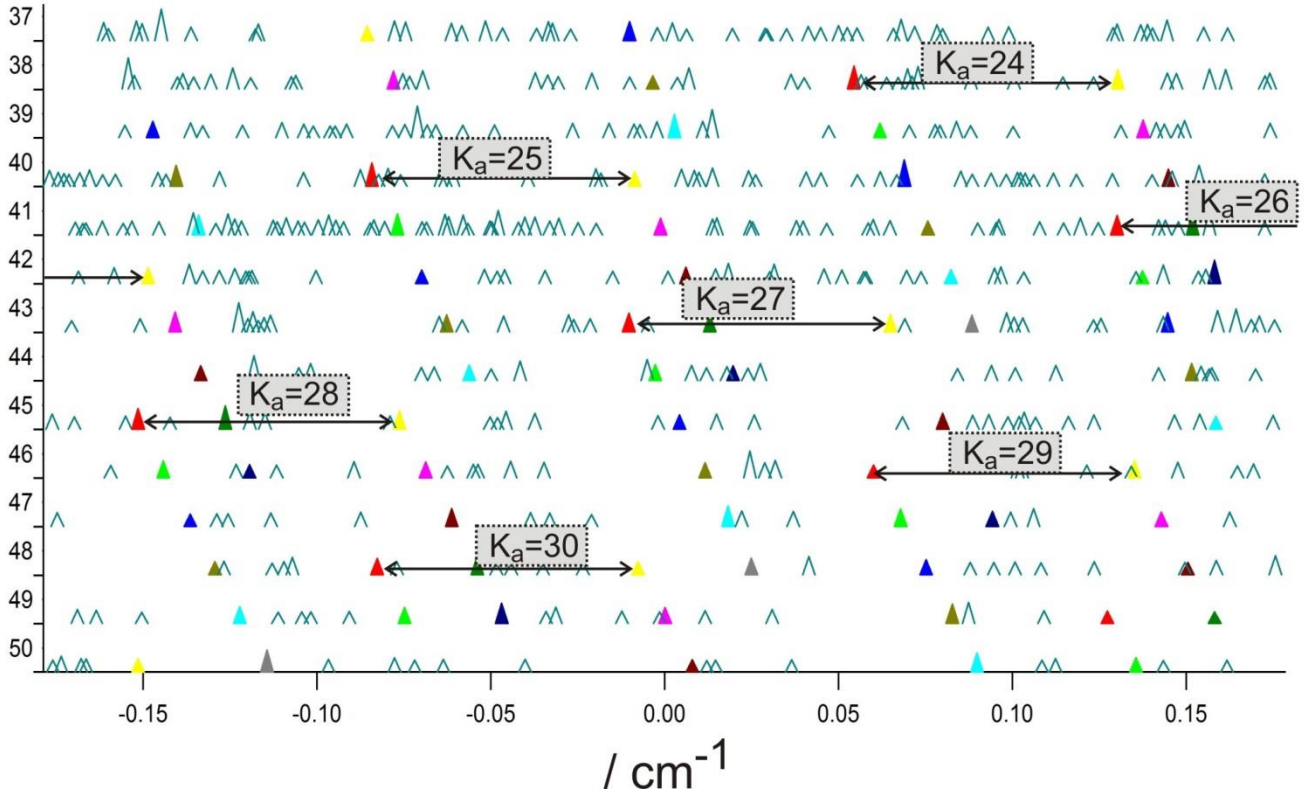

Figure 8: A closer look at a 0.25 cm^{-1} spectral region of the P branch of the ν_{10} band of SCB. The simulation (lower trace) shows the expected *a*-type rotation-vibration (green, purple) and *c*-type rotation-vibration-inversion (red, blue) transitions in this region.

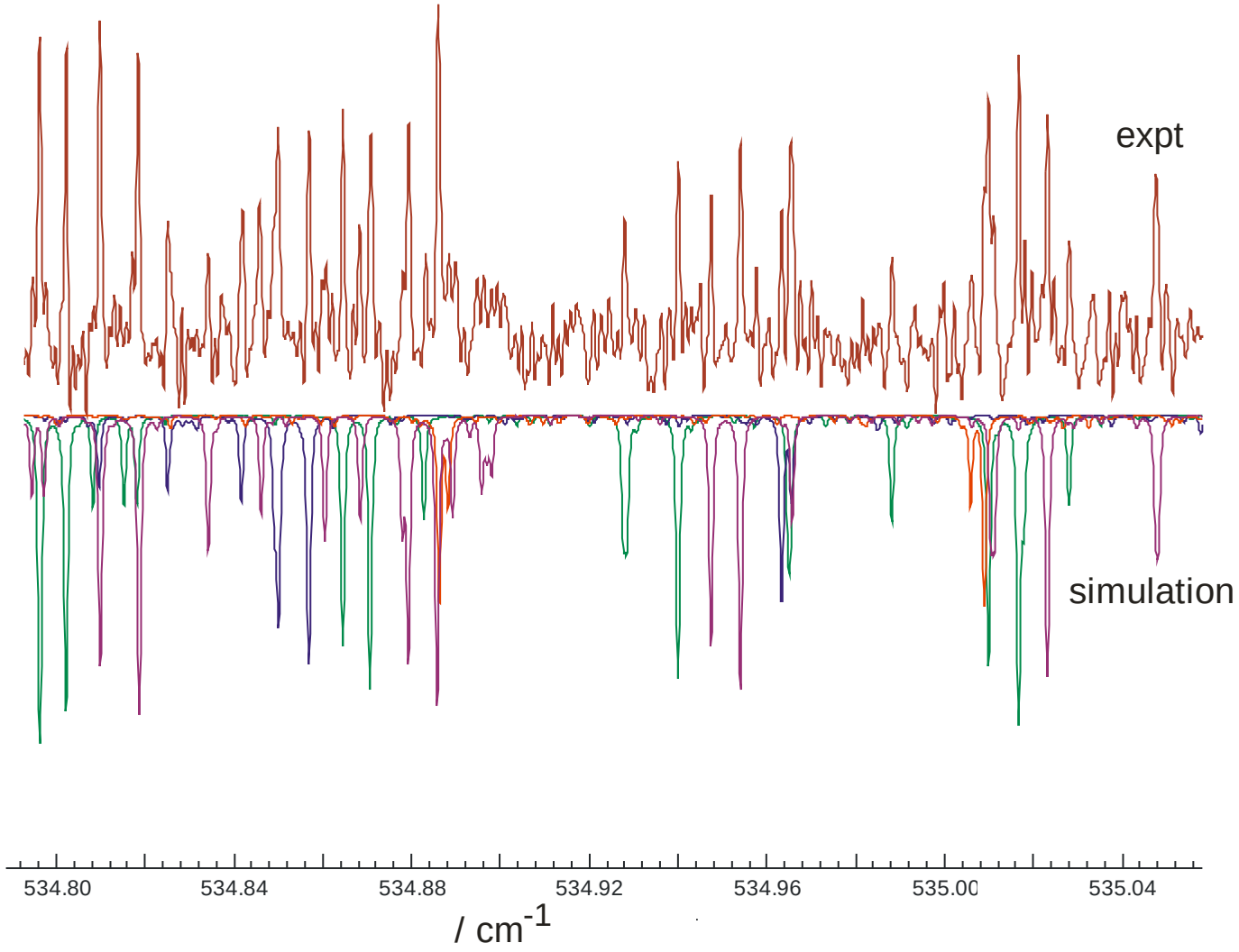

Figure 9: Overview spectrum showing band contour of the ν_{14} α-CH_2 rocking mode of SCB at ~737 cm^{-1}. This vibration is IR forbidden and the spectrum reflects the symmetry-allowed rotation-vibration-inversion transitions associated with this mode.

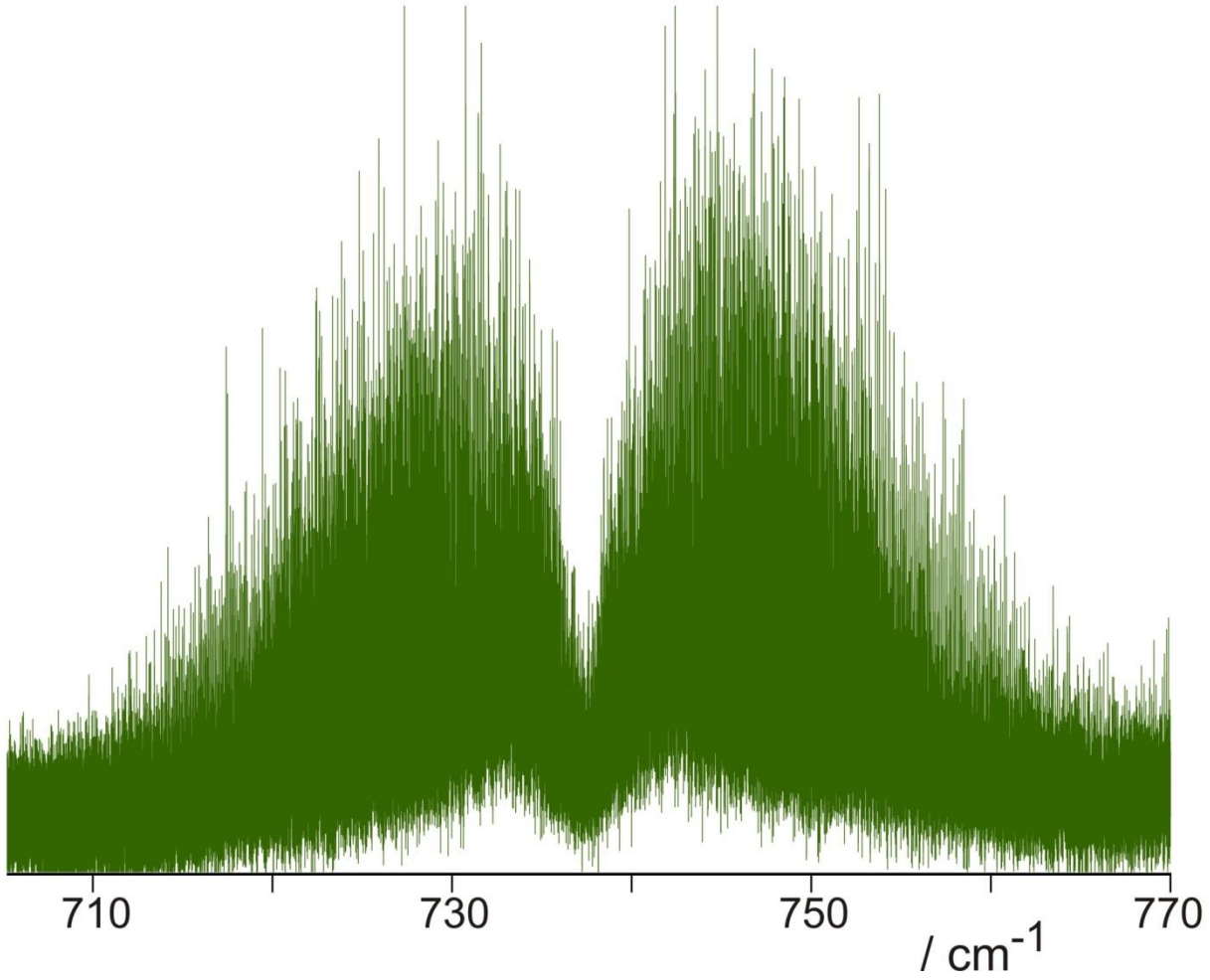

References

[1] Badran, I.; Forster, T. D.; Roesler, R.; Shi, Y. J. Competition of Silene/Silylene Chemistry with Free Radical Chain Reactions Using 1-Methylsilacyclobutane in the Hot-Wire Chemical Vapor Deposition Process. **2012**, J. Phys. Chem A, 116, 10054-10062.

[2] Avakyan, V. G.; Bukalov, S. S.; Aysin, R. R.; Leites, L. A. Unstable, 1,1,2,2-Tetramethyl-1,2-disilacyclobutane and Its Polymerization: Vibrational Spectroscopy and Quantum-Chemistry Study. Organometallics. **2012**, 31, 7063-7073.

[3] Cai, Z. J.; Shi, Y. J. On the Geometric Structure, Puckering Potential and Electronic Transitions of Monosilacyclobutanes and Disilacyclobutanes- A Theoretical Study. J. Mol. Spectrosc. **2011**, 267, 178-185.

[4] Tong, L.; Shi, Y. J. Decomposition of 1,1-Dimethyl-1-silacyclobutane on a Tungsten Filament-Evidence of Both Ring C-C and Ring Si-C Bond Cleavages. J. Mass Spectrometry. **2010**, 45, 215-222.

[5] Shi, Y. J.; Lo, B.; Tong, L.; Li, X.; Eustergerling, B. D.; Sorensen, T. S. In situ Diagnostics of the Decomposition of Silacyclobutane on a Hot Filament by Vacuum Ultraviolet Laser Ionization Mass Spectrometry. J. Mass. Spectrom. **2007**, 42, 575-583.

[6] Malloy, T. B. Far-infrared Spectra of Ring Compounds: A Semi-rigid Model for the Ring-Puckering Vibration in Some Pseudo-four-membered Ring Molecules. J. Mol. Spectrosc. **1972**, 44, 504–535.

[7] Legon, A. C. Equilibrium Conformations of Four- and Five-membered Cyclic Molecules in the Gas Phase: Determination and Classification. Chem. Rev. **1980**, 80, 231-262.

[8] Laane, J. Spectroscopic Determination of Ground and Excited State Vibrational Potential Energy Surfaces. Int. Rev. Phys. Chem. **1999**, 18, 301–341.

[9] van Wijngaarden, J.; Chen, Z.; van Dijk, C. W.; Sorenson, J. L. Pure Rotational Spectrum and Ring Inversion Tunnelling of Silacyclobutane, J. Phys. Chem A. **2011**, 115, 8650-8655.

[10] Chen, Z.; van Wijngaarden, J. Synchrotron-based Far Infrared Study of the Rotation-Vibration-Inversion Spectrum of Silacylcobutane Below 500 cm^{-1}: the ν_{29} and ν_{30} Bands. J. Chem. Phys. **2013**, 139, 244305.

[11] Laane, J.; Lord, R. C. Far-Infrared Spectra of Ring Compounds. III. Spectrum, Structure, and Ring-Puckering Potential of Silacylcobutane, J. Chem. Phys. **1968**, 48, 1508-1513.

[12] Pringle, W. C. P. Microwave Spectrum, Vibration-Rotation Interaction, ad Ring Puckering Vibration in Silacyclobutane and Silacyclobutane-1,1-d_2, J. Chem. Phys. **1971**, 54, 4979 -4988.

[13] McKellar, A. R. W. High-Resolution Infrared Spectroscopy with Synchrotron Sources, J. Mol. Spectrosc. **2010**, 262, 1-10.

[14] Chen, Z.; van Wijngaarden, J. The ν_{21} Ring Puckering Mode of 3-Oxetanone: A Far Infrared Spectroscopic Investigation Using Synchrotron Radiation, J. Mol. Spectrosc. **2012**, 279, 31-36.

[15] Zaporozan, T.; Chen Z; van Wijngaarden, J. High Resolution Fourier Transform Infrared Spectra and Analysis of the ν_{14}, ν_{15} and ν_{16} Bands of Azetidine, J. Mol. Spectrosc. **2010**, 264, 105-110.

[16] Laane, J. Synthesis of Silacyclobutane and Some Related Compounds. J. Am. Chem. Soc. **1967**, 89, 1144-1147.

[17] Laane, J. Vibrational Spectra and Normal-Coordinate Analyses of Silacyclobutanes, Spectrochim. Acta, **1970**, 26A, 517-540.

[18] Al-Saadi, A. A.; Laane, J. Structure, Vibrational Spectra, and DFT and *ab Initio* Calculations of Silacyclobutanes, Organometallics **2008**, 27, 3435-3443.

[19] Pickett, H. M. The Fitting and Prediction of Vibration-Rotation Spectra with Spin Interactions. J. Mol. Spectrosc. **1991**, 148, 371-377.

[20] Neese, C. F. Loomis-Wood Add-In (LWA) for Igor Pro, Version 2.0; 56th Ohio State University International Symposium on Molecular Spectroscopy. **2001**. Columbus,OH,June,20−24,2005, http://fermi.uchicago.edu/freeware/LoomisWood.shtml.

[21] IGOR Pro software, WaveMetrics Inc., Lake Oswego, OR USA, **2008**.